Heliyon 10 (2024) e30947

Contents lists available at ScienceDirect

Heliyon

journal homepage: www.cell.com/heliyon

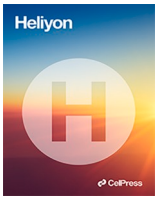

Research article

Megalin-targeted acetylcysteine polymeric prodrug ameliorates ischemia-reperfusion-induced acute kidney injury

Hao-Le Huang [a,*], Na Cheng [a], Can-Xin Zhou [a], Jing Liang [b]

[a] Department of Nephrology, the Affiliated People's Hospital of Ningbo University, Ningbo, 315040, China
[b] Department of Pharmacy, Zhejiang Hospital, Hangzhou, 310013, China

ARTICLE INFO

Keywords:
Acute kidney injury
Acetylcysteine
Low molecular weight chitosan
Renal tubular epithelial cells

ABSTRACT

Acute kidney injury (AKI), a condition associated with reactive oxygen species (ROS), causes high mortality in clinics annually. Active targeted antioxidative therapy is emerging as a novel strategy for AKI treatment. In this study, we developed a polymeric prodrug that targets the highly expressed Megalin receptor on proximal tubule cells, enabling direct delivery of N-Acetylcysteine (NAC) for the treatment of ischemia reperfusion injury (IRI)-induced AKI. We conjugated NAC with low molecular weight chitosan (LMWC), a biocompatible and biodegradable polymer consisting of glucosamine and N-acetylglucosamine, to enhance its internalization by tubular epithelial cells. Moreover, we further conjugated triphenylphosphonium (TPP), a lipophilic cation with a delocalized positive charge, to low molecular weight chitosan-NAC in order to enhance the distribution of NAC in mitochondria. Our study confirmed that triphenylphosphonium-low molecular weight chitosan-NAC (TLN) exhibits remarkable therapeutic effects on IRI-AKI mice. This was evidenced by improvements in renal function, reduction in oxidative stress, mitigation of pathological progress, and decreased levels of kidney injury molecule-1. These findings suggested that the polymeric prodrug TLN holds promising potential for IRI-AKI treatment.

1. Introduction

Acute kidney injury (AKI) is a serious global health issue characterized by a rapid decline in renal function, resulting in high mortality and morbidity rates [1]. The incidence of AKI is increasing and can be caused by various factors, including trauma, sepsis, surgery, nephrotoxic drugs, and ischemia-reperfusion injury (IRI), which is one of its main causes [2]. IRI can lead to cell necrosis and apoptosis, resulting in impaired renal function. There are several molecular mechanisms involved in IRI, including the production of oxygen free radicals, cytokines, and chemical factors triggered by ischemia-reperfusion. The accumulation of reactive oxygen species (ROS) during ischemia-reperfusion, coupled with a decrease in endogenous antioxidant substances, contributes to the sharp increase in ROS levels in the body, which is a significant cause of IRI [3]. Additionally, reperfusion is associated with the occurrence of inflammatory reactions, characterized by the production of inflammatory factors in the tissue and the aggregation of neutrophils. The excessive production of oxidants and pro-inflammatory mediators leads to extensive cell death in the reperfusion site tissue, manifesting as necrosis and programmed apoptosis, ultimately resulting in post-ischemic renal failure. Presently, clinical interventions for AKI patients mainly consist of renal replacement therapy and nutritional supplementation [4]. Despite several pharmacologic therapies, such as diuretics, vasoactive drugs, and growth factors being reported in animal models and preliminary clinical studies, no

* Corresponding author.
E-mail address: jj_dr@sina.com (H.-L. Huang).

https://doi.org/10.1016/j.heliyon.2024.e30947
Received 7 January 2024; Received in revised form 8 May 2024; Accepted 8 May 2024
Available online 9 May 2024

effective therapy has yet been established. Consequently, there is an urgent need for novel therapeutic strategies for AKI.

Renal tubular epithelial cells (TECs) are a crucial cell type in renal tubules, forming a continuous tubular structure that lines the walls of the tubules [5]. They play a significant role in urine production and concentration, as well as the regulation of water and electrolyte excretion and reabsorption. TECs achieve this by transporting ions and molecules across their cell membranes using specific transport channels and proteins. They also facilitate the removal of waste and drugs from the blood to the urine, aiding in the elimination of harmful substances from the body. Therefore, TECs are key players in kidney disease and injury. During IRI, there is a disruption in the blood and oxygen supply to the renal tissue. This leads to abnormal electron transport within the mitochondrial respiratory chain in TECs and a rapid overproduction of ROS in mitochondria. Consequently, oxidative stress reactions are exacerbated. Excess ROS combine with calcium ions in mitochondria, causing the opening of mitochondrial inner membrane exchange channels and subsequent swelling and rupture of mitochondria. This release of pro-apoptotic factors further activates the expression of apoptotic proteins, ultimately inducing TEC apoptosis [6]. Therefore, the effective distribution of ROS scavengers in renal tissue is crucial for antioxidant therapy in IRI-AKI. It is essential to achieve active targeted drug delivery to renal TECs and intracellular mitochondria, thereby increasing the concentration of therapeutic drugs in these specific areas.

TECs express a significant amount of Megalin receptors that act as transporters to facilitate protein endocytosis from the urine that have been filtered by the glomerulus. Megalin also enables various oligocationic compounds such as aminoglycosides and toxins to be retained with the help of cubilin receptor protein [7,8]. As the epithelial cells and the tubular fluid are separated by no endothelial layer, TECs in the kidney can be targeted through the tubular lumen. However, it is essential to note that the glomerulus provides a barrier for the tubular lumen, restricting the size of drug carriers that can pass through. Typically, particles with a hydrodynamic diameter below 5–7 nm are quickly excreted, excluding most drug carriers such as liposomes and antibodies that have sizes between 10 and 200 nm. Nevertheless, some low molecular weight carriers such as protein-based, polymeric, and folate-conjugated carriers have shown success in specifically targeting drugs to the kidney [9,10].

N-Acetylcysteine (NAC), an antioxidant compound, is a colorless, water-soluble amino acid that stabilizes cell membranes and protects collagen and endothelium. NAC plays an important role in maintaining human health. It can resist free radical damage, reduce inflammation and damage in the body, and protect the health of important organs such as the brain, liver and cardiovascular system [11]. Here, we developed a polymeric prodrug targeting the megalin receptor, which enables direct delivery of NAC to renal tissues. This polymeric prodrug design offers significant therapeutic properties, including an extended half-life, improved bioavailability, and targeted delivery to specific cells or tissues. Our polymeric carrier utilizes low molecular weight chitosan (LMWC), a biocompatible and biodegradable polymer consisting of glucosamine and N-acetylglucosamine. LMWC has been shown to be selectively absorbed by TECs, making it an effective carrier for treating renal diseases. To enhance the accumulation of NAC in the mitochondria, triphenylphosphonium (TPP), a cation with sufficient lipophilicity and a delocalized positive charge, was further conjugated to the polymeric prodrug (LN). This conjugation reduces the free energy change when the polymeric prodrug moves from an aqueous environment to a hydrophobic one, thus promoting its accumulation in response to the mitochondrial membrane potential.

TLN is designed to deliver the antioxidant NAC to both renal TECs and intracellular mitochondria. Its goal is to reduce ROS levels in the renal tissues of IRI-AKI. Our study confirmed that TLN has remarkable therapeutic effects on IRI-induced AKI model animals, as reflected by renal function, reduction in oxidative stress, and kidney injury molecule. Thus, this targeted drug delivery strategy presents a novel therapeutic approach for AKI.

2. Materials and methods

2.1. Synthesis and characterization of TLN

TPP, DCC and 4-DMAP were dissolved in anhydrous dimethylsulfoxide (DMSO) and stirred at 60 °C for 1 h to activate the carboxyl of TPP. LMWC in anhydrous DMSO (5 mL) was then added dropwise over 10 min, and sequentially stirred for 48 h at 60 °C. After the reaction, the products were placed in a dialysis bag (MWCO 1000) and dialyzed with deionized water for 48 h. The solution was filtered, and the filtrate was freeze-dried to obtain TL. Then, TL, NAC, DCC and 4-DMAP were dissolved in anhydrous DMSO, and stirred for 48 h at 60 °C. After the reaction, the products were placed in a dialysis bag (MWCO 1000) and dialyzed with deionized water for 48 h. The solution was filtered, and the filtrate was freeze-dried to obtain TLN.

TLN was characterized by ^{1}H and ^{31}P NMR spectrometer. The substitution ratio of TPP in TPP-LMWC-NAC was calculated according to the area of characteristic peaks. The drug loading of NAC in TLN was measured by alkali hydrolysis and subsequent high performance liquid chromatography (HPLC) assay.

In vitro release of NAC from TLN was investigated using the dialysis method. Briefly, 1 mL TLN (5 mg/mL) were loaded into dialysis bag (MWCO 1000) and immersed into 40 mL of various pH buffer solutions (pH 7.4). The experiments were performed under horizontal shaking (60 rpm) at 37 °C. At predetermined time intervals, 1 mL samples were collected and replenished with fresh medium. The content of NAC was measured using HPLC method.

2.2. ROS scavenging assays

2.2.1. DPPH

Different concentrations of TLN, NAC as control, were first mixed in equal volumes with 125 μM of DPPH ethanol solution, and after 30 min of complete reaction, the absorption of DPPH at 517 nm was tested. DPPH scavenging efficiency (%) = $((A_{DPPH}\text{-}A_{Sample})/A_{DPPH}) \times 100$ %. A_{DPPH} represented the absorbance of free DPPH. A_{Sample} represented the absorbance of DPPH with the addition of TLN

or NAC.

2.2.2. ABTS

ABTS free radicals were obtained by activating 7 mM ABTS with 2.45 mM potassium persulfate overnight, and then TLN was mixed with ABTS free radicals for 10 min to test the absorption of ABTS free radicals at 734 nm. ABTS scavenging efficiency (%) = $((A_{ABTS} - A_{Sample})/A_{ABTS}) \times 100$ %. A_{ABTS} represented the absorbance of free ABTS. A_{Sample} represented the absorbance of ABTS with the addition of TLN or NAC.

2.2.3. PTIO

400 mL of PTIO· (0.5 mg/mL) solution was added in 4 mL PBS containing different concentrations of TLN, free NAC as control. After 24 h, the absorption of the solutions at 557 nm were detected, and the clearance rate of PTIO· was calculated.

2.3. Cellular uptake

TLN was conjugated with fluorescein for cellular uptake studies. In brief, TLN, fluorescein, DCC and 4-DMAP were dissolved in anhydrous DMSO, and stirred for 48 h at 60 °C. After the reaction, the products were placed in a dialysis bag (MWCO 1000) and dialyzed with deionized water for 48 h. The solution was filtered, and the filtrate was freeze-dried to obtain fluorescein-conjugated TLN (TLN (F)).

HK-2 cells were seeded in a 12-well plate at 5×10^4 cells per well and incubated for 24 h. Then, H_2O_2 or PBS-induced cells were incubated with TLN (F) for 1 and 6 h, respectively, LN (F) as control. After that, the supernatant was removed and washed with PBS, cells were fixed with cold methanol and visualized by the inverted fluorescent microscope.

2.4. Colocalization analysis

Fluorescence imaging and colocalization analysis were used to investigate whether TLN entered cells through Megalin receptor. Sterilized coverslips were placed in a 12-well cell culture plate, and HK-2 cells were seeded at a density of 1×10^5 cells per well and incubated for 24 h. Then, TLN (F) was added and incubated for 6 h. After that, the supernatant was removed and washed with PBS, cells were fixed with cold methanol, and then incubated with anti-Megalin antibody (1 : 200, Proteintech) at 4 °C overnight, followed by Alexa Fluor 555-labeled second antibody ($E_X = 555$ nm, $E_M = 565$ nm) at room temperature for 1 h. The internalization of TLN (F) and the expression of Megalin antibody was visualized using the inverted fluorescent microscope, and the colocalization analysis was performed by ImageJ software.

Colocalization analysis between TLN (F) and mitochondria was performed to assess the mitochondria-targeting activity of TLN. Sterilized coverslips were placed in a 12-well cell culture plate, and HK-2 cells were seeded at a density of 1×10^5 cells per well and incubated for 24 h. Then, TLN (F) was added and incubated for 6 h. After that, the supernatant was removed and washed with PBS, cells were incubated with MitoTracker® Red CMXRos at 37 °C for 30 min. After washed, cells were fixed with cold methanol, sealed and observed using a laser scanning confocal microscope, and the colocalization analysis was performed by ImageJ software.

2.5. Cell viability

To investigate whether TLN protects HK-2 cells from oxidative stress damage, CCK-8 assay was used to assess cell viability. Briefly, HK-2 cells were seeded in a 96-well plate at 1×10^4 cells per well and incubated for 24 h. Cells were exposed to H_2O_2 (200 μM) for 2 h, and then treated with TLN for 24 h, free NAC and LN as control. After that, CCK-8 solution was added and incubated at 37 °C for 1 h. The absorbance at 570 nm was measured with a microplate reader, and the cell viability was calculated.

2.6. MitoSOX and mitochondrial membrane potential

To effect of TLN on the changes of mitochondrial superoxide in H_2O_2-treated HK-2 cells was investigated as previously described. HK-2 cells were seeded in a 12-well plate at 5×10^5 cells per well and incubated overnight. Cells were exposed to H_2O_2 (200 μM) for 2 h, and then treated with TLN for 24 h, free NAC and LN as control. After washed with Hank's balanced salt solution, cells were incubated with 500 nM MitoSOX™ Red reagent for 30 min at 37 °C in the dark. The fluorescence signal of mitochondrial superoxide was observed by the inverted fluorescent microscope.

2.7. Mitochondrial membrane potential

To effect of TLN on the changes of mitochondrial membrane potential in H_2O_2-treated HK-2 cells was detected by JC-1 probe. HK-2 cells were seeded in a 6-well plate at 1×10^5 cells per well and incubated overnight. Cells were exposed to H_2O_2 (200 μM) for 2 h, and then treated with TLN for 24 h, free NAC and LN as control. The medium was removed, cells were incubated with fresh medium and JC-1 working solution (1 mL) for 20 min at 37 °C in the dark. After incubation, cells were washed with JC-1 buffer twice, incubated with fresh medium and the observed by the inverted fluorescent microscope.

2.8. Biodistribution

To investigate the distribution of TLN, IRI-AKI mice were injected intravenously with TLN (F). At 1 h, 6 h and 12 h after administration, mice were sacrificed, and their organs (heart, liver, spleen, lung and kidney) were collected, sliced, embedded, and sealed. The fluorescence signal of TLN (F) in every organ was visualized by the inverted fluorescent microscope.

2.9. IRI-induced AKI animal model and treatment

The Balb/c mice (20–25 g) were obtained from SpePharm (Beijing) Biotechnology Co., Ltd., and used in this study. After the mice

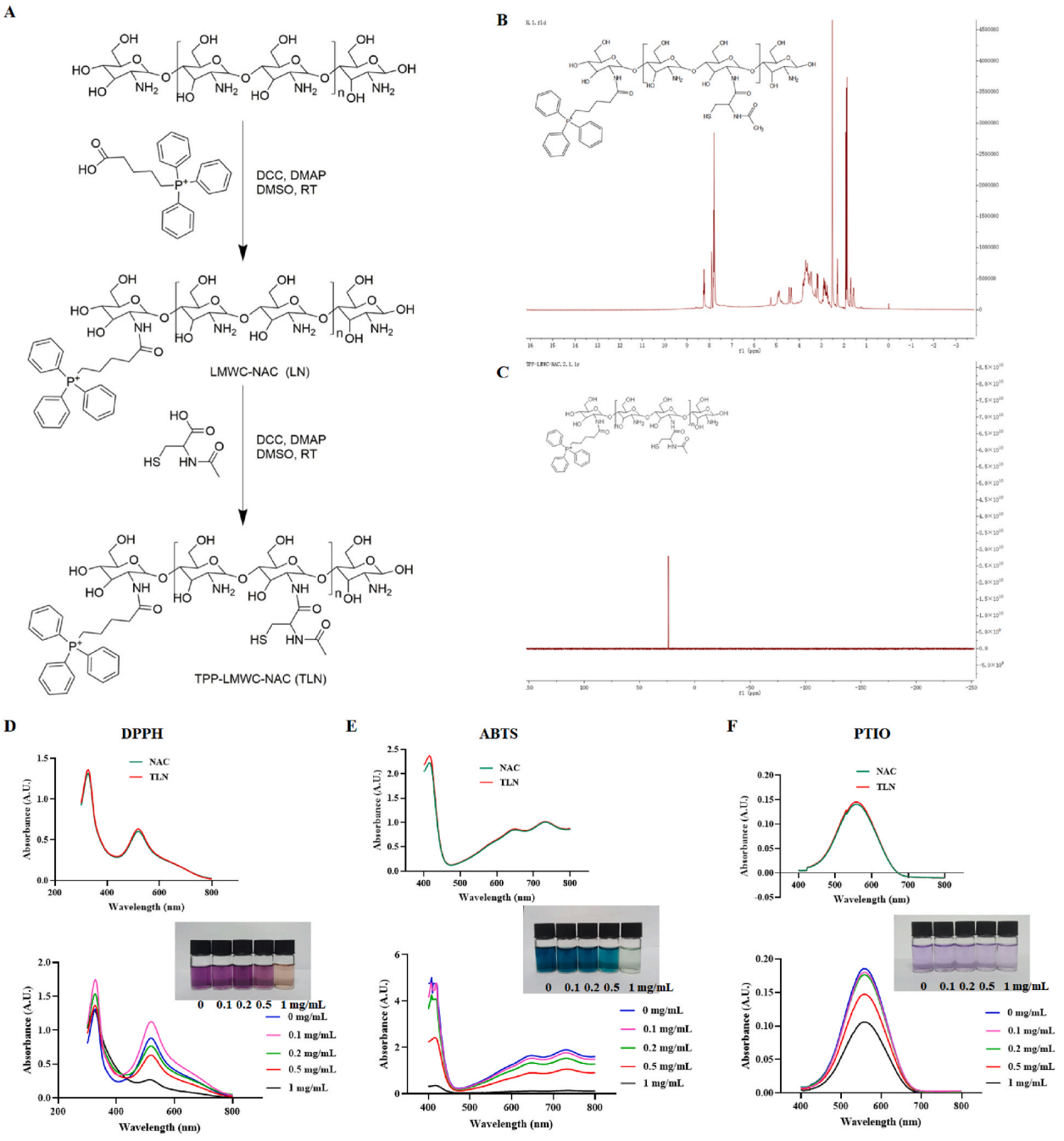

Fig. 1. The synthesis and characterization of TLN. (A) The synthetic route of TLN. (B) ^{1}H NMR spectrum of TLN. (C) ^{31}P NMR spectrum of TLN. The effects of TLN on the changes of DPPH (D), ABTS (E) and PTIO (F).

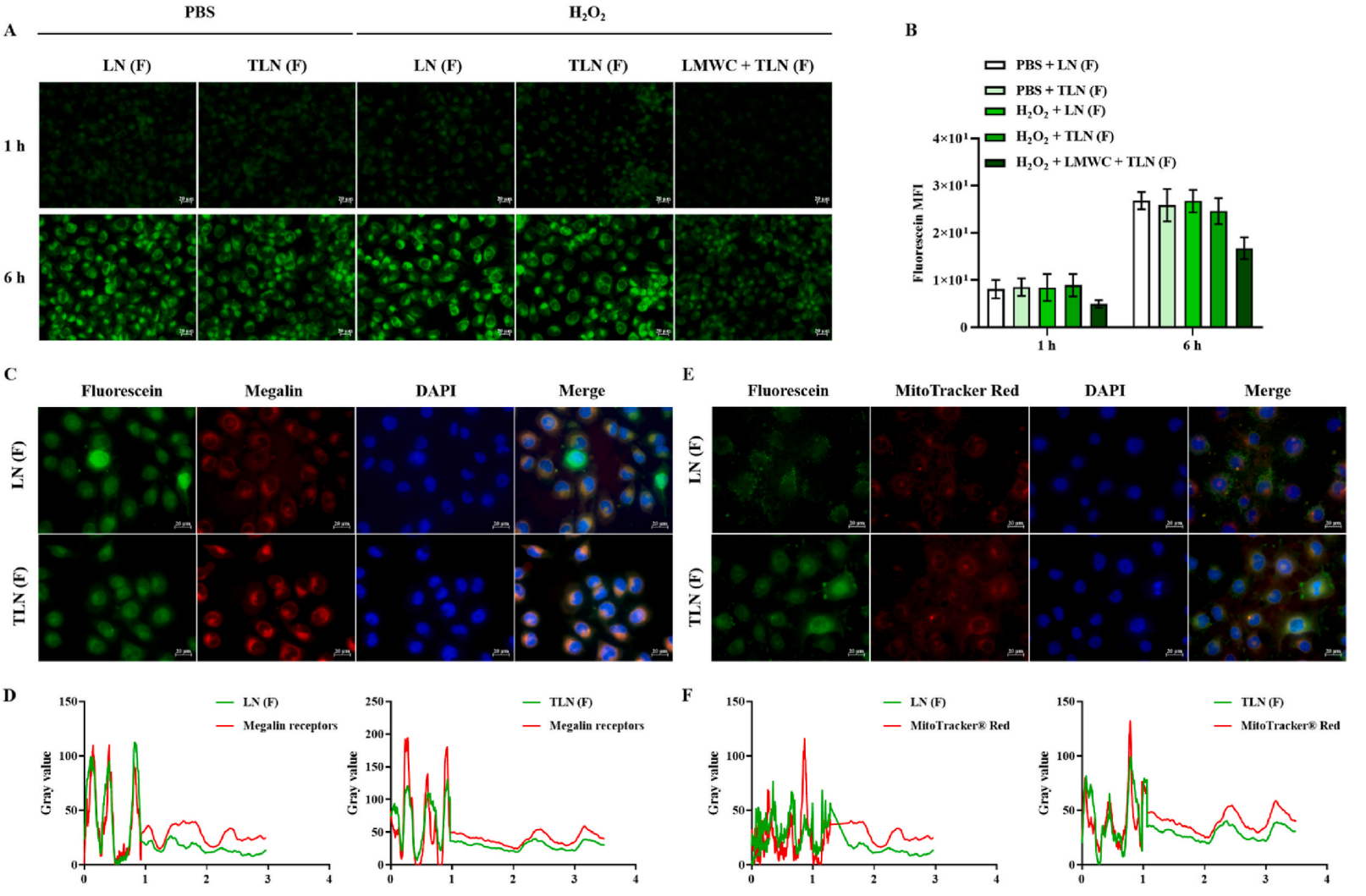

Fig. 2. The internalization and mitochondrial distribution of TLN. (A) The internalization behaviors of TLN (F) in PBS- or H2O2-induced HK-2 cells, LN (F) as control. (B) Semiquantitative analysis on intracellular fluorescence signals. (C) Representative fluorescent images of colocalization of TLN (F) with Megalin receptors expressed on HK-2 cells, and (D) the level of overlay of TLN (F) and Megalin receptors, LN (F) as control. (E) Representative fluorescent images of colocalization of TLN (F) with mitochondria in HK-2 cells, and (F) the level of overlay of TLN (F) and mitochondria, LN (F) as control. Scale bar = 20 μm.

were anesthetized with isoflurane, a midline incision was made to open up the abdominal cavity. Both renal pedicles were clamped with a micro clip for a duration of 45 min while maintaining body temperature on a temperature-regulated table. The sham group underwent a similar procedure without the application of the clip [12].

Mice were randomly divided into five groups: (1) Sham group; (2) IRI group; (3) IRI + NAC group; (4) IRI + LN group; (4) IRI + TLN group. Blood samples were collected from the retro-orbital venous plexus at the scheduled times after reperfusion. At 24 h after reperfusion, mice were sacrificed and renal tissues were collected for measurements.

2.10. Renal function

The changes in renal function were assessed via determining serum creatinine (Scr) and blood urea nitrogen (BUN) levels in AKI mice after treated with TLN. Serum samples were measured by using an automated analyzer (Roche Diagnostics, Germany).

2.11. Oxidative stress and pro-inflammatory cytokines

Superoxide dismutase (SOD) and malondialdehyde (MDA) in renal tissues were detected using commercial kits (Nanjing jiancheng Bioengineering Institute, Nanjing, China) according to the manufacturer's instructions.

2.12. Histologic evaluation

To assess the renal histopathological changes in AKI mice, renal sections were fixed with 4 % paraformaldehyde, embedded in paraffin, cut into 3 μm sections, and stained with hematoxylin and eosin (H&E). The H&E staining sections were observed using a light microscopy. The renal sections were incubated with anti-KIM-1 antibody to detect the expression of kidney injury molecular-1 (KIM-1) in renal tissues of AKI mice after treated with TLN free NAC and LN as control. CM-H_2DCFDA injection was used to detect the generation of ROS in renal tissues of AKI mice. After treatment, the mice were anesthetized using chloral hydrate. Then, they were injected with 100 μg of CM-H_2DCFDA into the renal circulation. After 45 min, the kidneys were collected and soaked in 4 % paraformaldehyde for 24 h. Next, the renal tissue was treated with 20 % sucrose for 12 h. It was then frozen in liquid nitrogen and cut into cryostat sections (5 μm) using a cabinet set at −20 °C. These sections were placed on adhesive slides and allowed to air-dry at room temperature for 3 min. Following this, the sections were washed in PBS, stained with DAPI, and captured using an inverted fluorescent microscope.

2.13. Statistical analysis

All values are reported as mean ± standard deviation (SD) unless otherwise stated. All statistical analysis was performed using Graphpad 8 software. The significant differences between the groups were analyzed by a Student's *t*-test, and $P < 0.05$ was considered significant.

3. Results and discussion

3.1. Characterization of TLN

The synthetic route of TLN was shown in Fig. 1A. TL was firstly synthesized via coupling amino group of LMWC with carboxyl group of TPP, and then NAC was conjugated to TL to obtain TLN. The ^{1}H spectrum of TLN was showed in Fig. 1B, S1, S2 and S3, the peak of TLN at 4.37 ppm belonged to NAC, suggesting that NAC was conjugated to LMWC. The ^{31}P spectrum of TLN was showed in Fig. 1B, S4, successful conjugation of TPP onto the backbone of LMWC was confirmed by the appearance of peak at 23.88 ppm. As determined by ^{1}H NMR, the molar ratio of TPP to LMWC in TLN was 1.4 : 1. The drug loading of NAC in TLN was 14.3 %. The *in vitro* release behaviors of TLN were detected in pH 7.4 PBS solution. As shown in Fig. S5, compared with free NAC, the release of NAC from TLN was prolonged. In addition, the release behaviors of LN and TLN were similar.

The *in vitro* antioxidant activity of TLN was examined, DPPH as antioxidant indicator. The absorption peak of DPPH at 517 nm, which serves as a characteristic feature, decreases or disappears when free radical scavengers are present. When we added the same concentration of NAC and TLN to the DPPH solution, the absorption of DPPH at 517 nm showed a significant decrease. This result suggested that grafting NAC onto LMWC did not affect its antioxidant activity. Moreover, TLN exhibited a dose-dependent antioxidant activity (Fig. 1D). In addition, TLN could scavenge ABTS and PTIO in a dose-dependent manner (Fig. 1E and F).

3.2. The internalization and mitochondrial distribution of TLN

The internalization of TLN by HK-2 cells was investigated by visualizing the intracellular fluorescence signal of fluorescein-conjugated TLN (TLN (F)) under an inverted fluorescent microscope. As shown in Fig. 2A and B, the increasing fluorescence signals (1 h *vs* 6 h) were gradually observed with the extension of incubation time, showing that TLN (F) exhibited excellent time-dependent cellular uptake ability. This finding is significant as it implies the efficient delivery of therapeutic cargoes into cells by drug delivery systems, which is crucial for NAC intervention. In addition, the internalization behaviors of TLN (F) in PBS- and H_2O_2-treated cells were similar, further suggesting that TLN was suitable for oxidative stress-damaged TECs. Interestingly, the addition of LMWC induced the increase of the average fluorescent intensity in HK-2 cells as reflected by the reduced intracellular fluorescent signals, suggesting

that Megalin receptor-mediated endocytosis in HK-2 was blocked competitively.

The Megalin receptor-mediated endocytosis of TLN (F) in HK-2 cells was confirmed via fluorescence colocalization analysis. As shown in Fig. 2C and D (overlay level), the presence of red fluorescent signals showed the Megalin receptors located on the cells, whereas the green signals indicated the internalized LN (F) or TLN (F). Results revealed that both TLN (F) and LN (F) had higher overlap with Megalin receptors (Pearson's correlation coefficient, $P = 0.89 \pm 0.07$ and 0.85 ± 0.08 for LN (F) and TLN (F)), indicating that the internalization behavior of TLN was through Megalin receptor-mediated endocytosis in HK-2 cells.

Mitochondrial dysfunction has been implicated in the development of IRI-AKI [13]. To effectively treat AKI, it is important to target the delivery of antioxidants to the mitochondria and reduce oxidative stress. In this study, the sub-cellular localization of TLN was examined to confirm its mitochondria-targeted properties. Mitochondria were labeled using MitoTracker Red probes. As shown in Fig. 2E and F (overlay level), the co-localization between TLN (F) and mitochondria was significantly higher compared to LN (F) ($P = 0.74 \pm 0.12$ and 0.35 ± 0.11 for TLN (F) and LN (F), respectively). These results demonstrated that TLN exhibited a high degree of targeting towards mitochondria, indicating its potential for mitochondria-targeted therapy and reversal of mitochondrial dysfunction.

3.3. Renal distribution of TLN

The expression of Megalin receptor in renal tissues of IRI-AKI mice was investigated using immunohistochemical staining. As

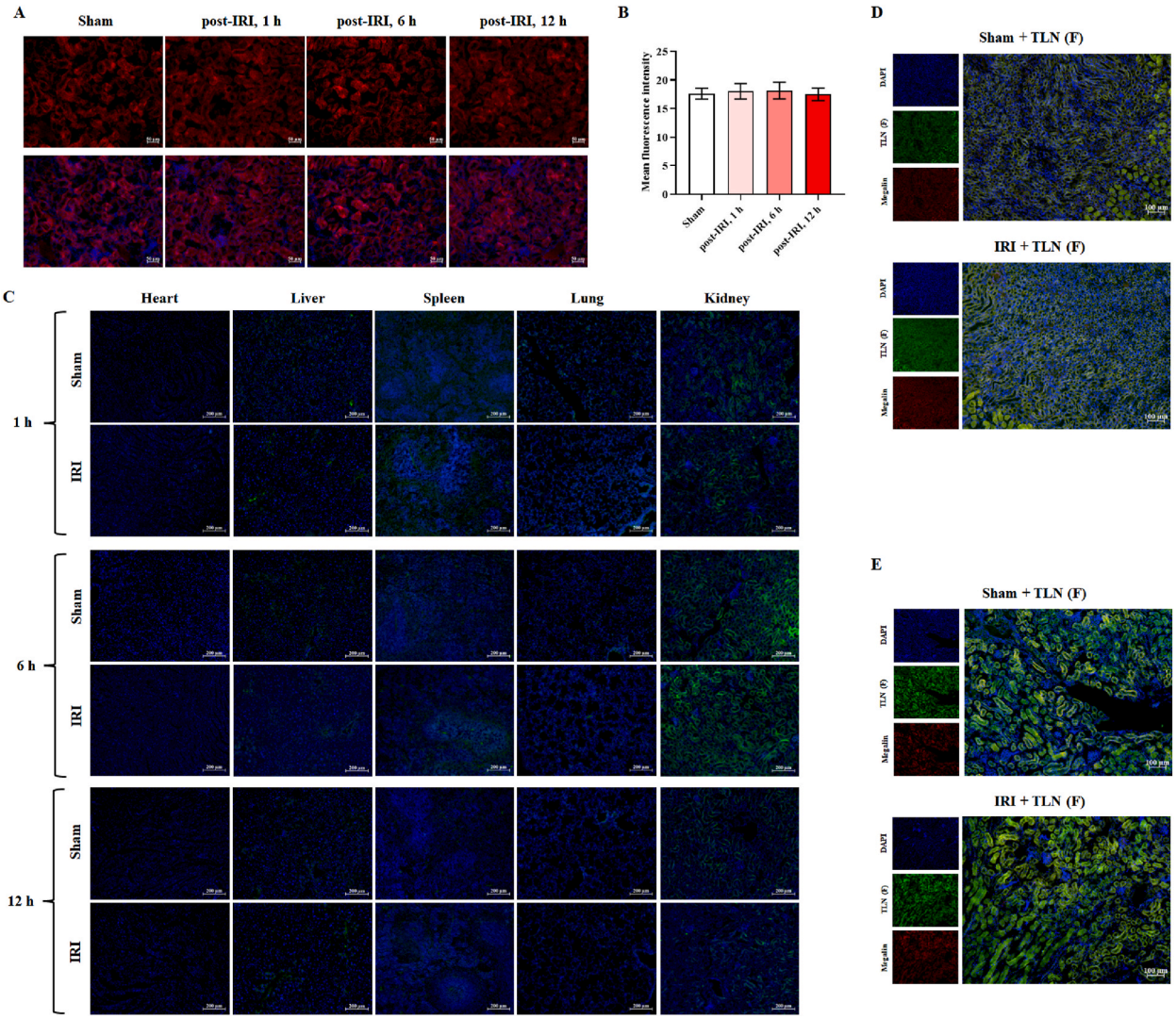

Fig. 3. The biodistribution of TLN IRI-AKI mice. (A) The expression of Megalin receptors in renal tissues of IRI-AKI mice at different time points, and (B) semi-quantitative analysis on the positive signals of Megalin receptors. Scale bar = 50 μm. (C) The biodistribution of TLN (F) in sham and IRI-AKI mice at 1 h, 6 h and 12 h after intravenous injection. Scale bar = 200 μm. (D) and (E) Representative fluorescent images of colocalization of TLN (F) with Megalin receptors in renal tissues of sham or IRI-AKI mice at 1 h and 6 h after intravenous injection. Scale bar = 100 μm.

shown in Fig. 3A and B (semi-quantitative analysis), the expression of Megalin receptors were no changes in different times after IRI, which provided the reasonable basis for the renal targeting therapy of TLN. Then, the biodistribution of TLN was examined in both sham and IRI-AKI mice after intravenous injection, at 1 h, 6 h and 12 h post-injection. The results, as illustrated in Fig. 3C, indicated the presence of TLN (F) in the renal tissues of both sham and IRI-AKI mice at 1 h after injection, suggesting that TLN exhibited rapid and efficient distribution in the kidneys. Furthermore, the renal distribution of TLN (F) was found to be further increased at 6 h post-injection. At 12 h post-injection, the fluorescence signals in the renal tissues of both sham and IRI-AKI mice was reduced in comparison to that at 6 h. Moreover, there was minimal distribution of TLN (F) observed in other tissues, including heart, liver, spleen, and lung. These findings clearly demonstrated the superior targeting capability of TLN towards renal tissues, suggesting its potential for targeted treatment of IRI-AKI. The observed increased and prolonged accumulation of TLN in the kidneys could be attributed to two factors. Firstly, TLN possessed good water solubility and low molecular weight, allowing it to rapidly reach renal tissues and enter the renal tubules via glomerular filtration. Secondly, TLN had the ability to specifically bind to Megalin receptors in renal proximal tubule epithelial cells, facilitating its uptake into these cells.

The colocalization analysis was also performed to detect the distribution of TLN in renal tissues of sham and IRI-AKI mice after intravenous injection, at 1 h and 6 h post-injection. As shown in Fig. 3D (1 h post-injection) and 3E (6 h post-injection), the fluorescence signal of TLN (F) had good overlap with that of Megalin receptors, suggesting that TLN was mainly accumulated in renal TECs.

3.4. TLN protects TECs from oxidative stress damages

Based on the *in vitro* ROS scavenging ability of TLN, we further investigated whether TLN protected HK-2 cells against H_2O_2-

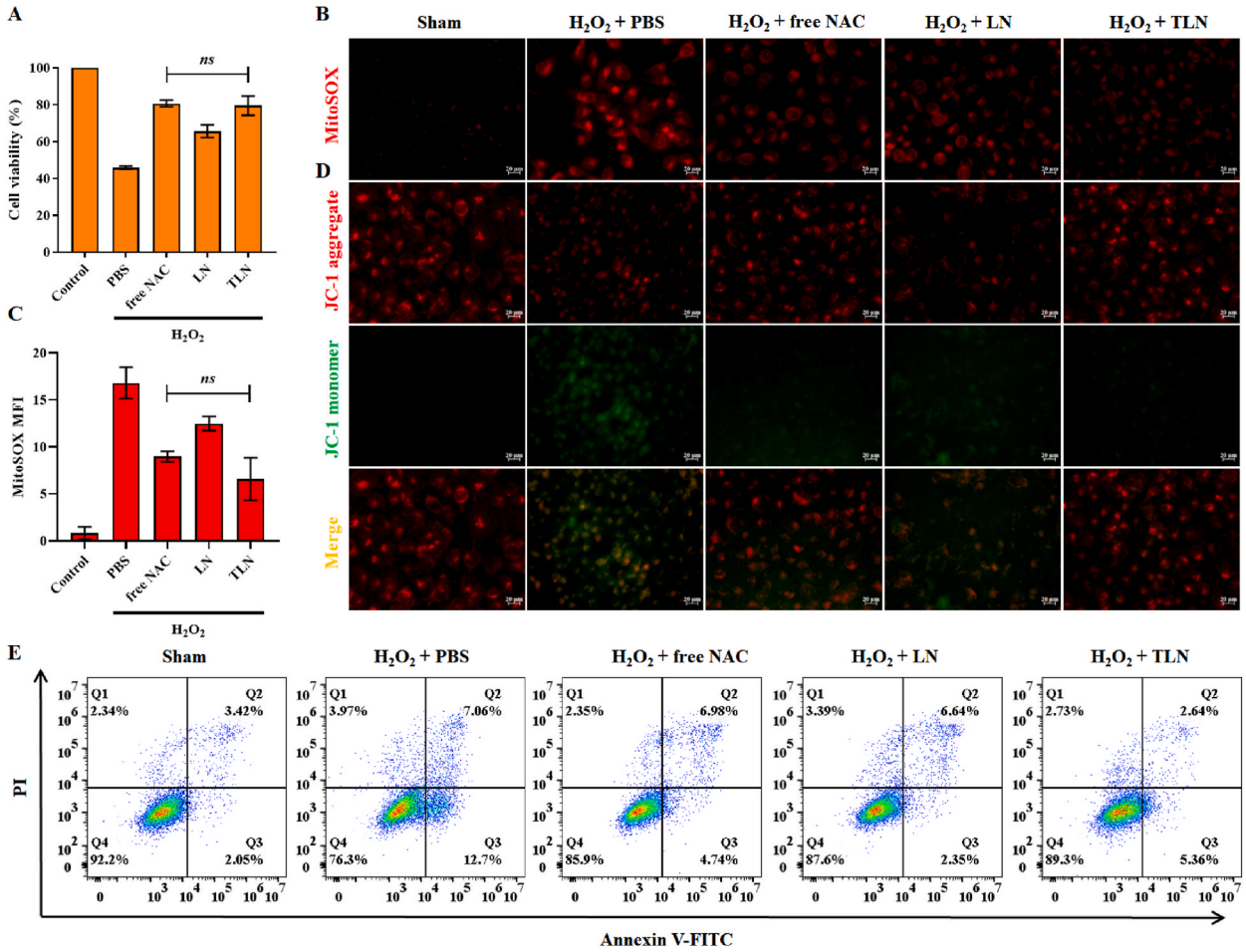

Fig. 4. TLN protects HK-2 cells from oxidative stress damages. (A) The cell viability of H_2O_2-induced HK-2 cells after treated with TLN, free NAC and LN as control. (B) and (C) The changes of mitochondrial ROS production in H_2O_2-induced HK-2 cells after treated with TLN, free NAC and LN as control, and semiquantitative analysis on fluorescence signals. (D) The changes of mitochondrial membrane depolarization in H_2O_2-induced HK-2 cells after treated with TLN, free NAC and LN as control. (E) The apoptosis of HK-2 cells was measured by flow cytometry. Data are mean ± SD, n = 3. Scale bar = 20 μm.

induced damage. Firstly, the cytotoxicity of TLN was assessed by CCK-8 assay. At 24 h, there was no considerable cytotoxicity observed, even when the concentration was increased up to 200 μg/mL (Fig. S6). Next, we developed models of oxidative stress induced by H_2O_2 to investigate the efficacy of TLN in scavenging ROS. Results from the CCK-8 assay (Fig. 4A) showed that TLN

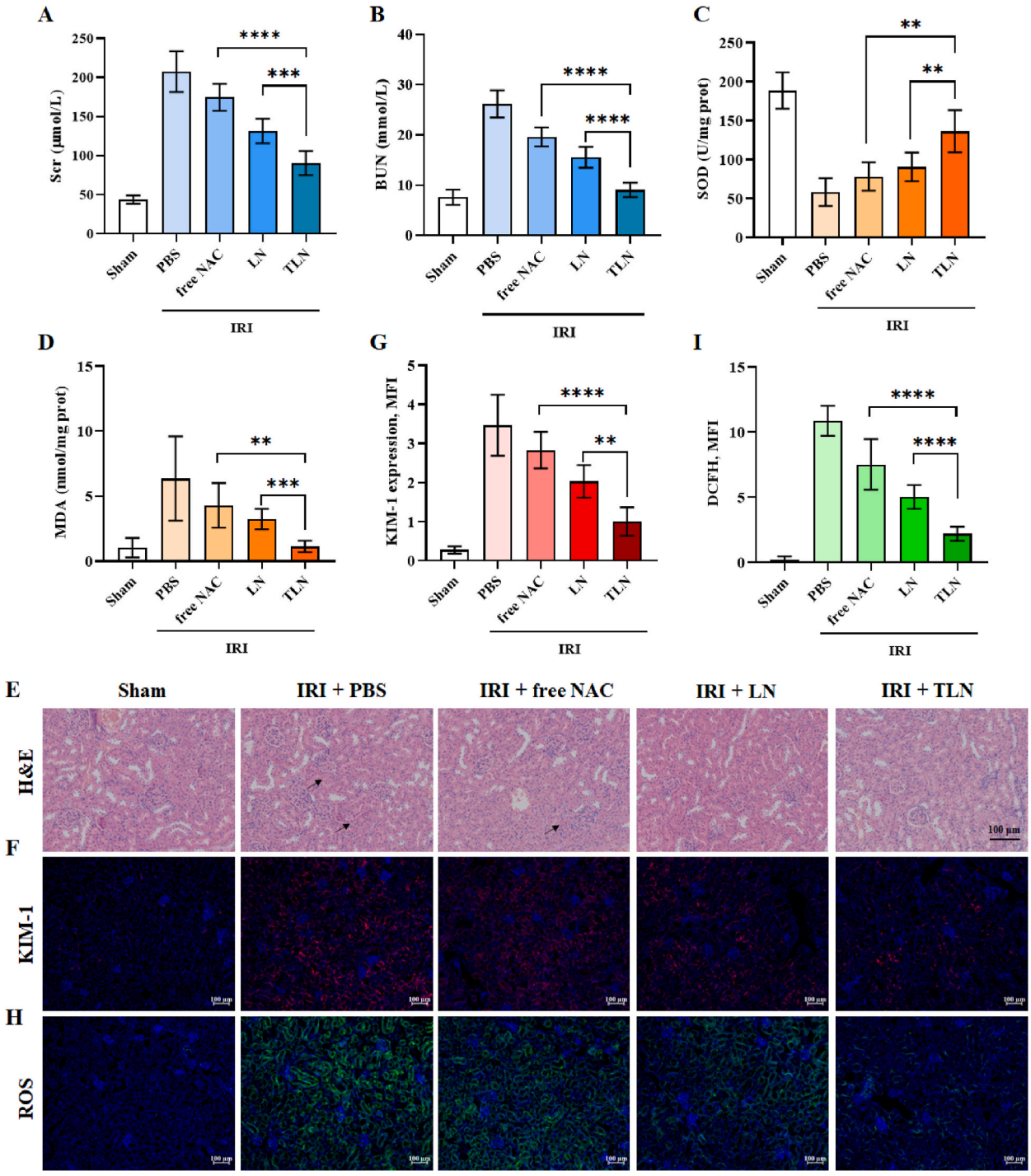

Fig. 5. TLN alleviates renal dysfunction of AKI mice. (A) and (B) The changes of Scr and BUN in IRI-AKI mice after treated with TLN, free NAC and LN as control. (C) and (D) The changes of Scr and BUN in renal tissues of IRI-AKI mice after treated with TLN, free NAC and LN as control. Data are mean ± SD, n = 6. (E) Representative H&E staining of renal tissues. (F) and (G) Representative KIM-1 staining sections of renal tissues, and semiquantitative analysis on ROS-positive fluorescence signals. (H) and (I) Representative ROS staining sections of renal tissues, and semi-quantitative analysis on KIM-1-positive fluorescence signals. Scale bar = 100 μm.

provided significant protection to HK-2 cells against damage caused by H_2O_2-induced oxidative stress.

The study investigated the ability of TLN to decrease mitochondrial ROS production in HK-2 cells using MitoSOX Red probe. Results (Fig. 4B and C) showed that the presence of H_2O_2 significantly increased the intracellular fluorescence signal, indicating a notable increase in ROS levels. However, treatment with TLN resulted in a substantial decrease in fluorescence intensity, which was lower compared to those treated with LN. This observation suggested that TLN exhibited a superior capability in reducing mitochondrial ROS

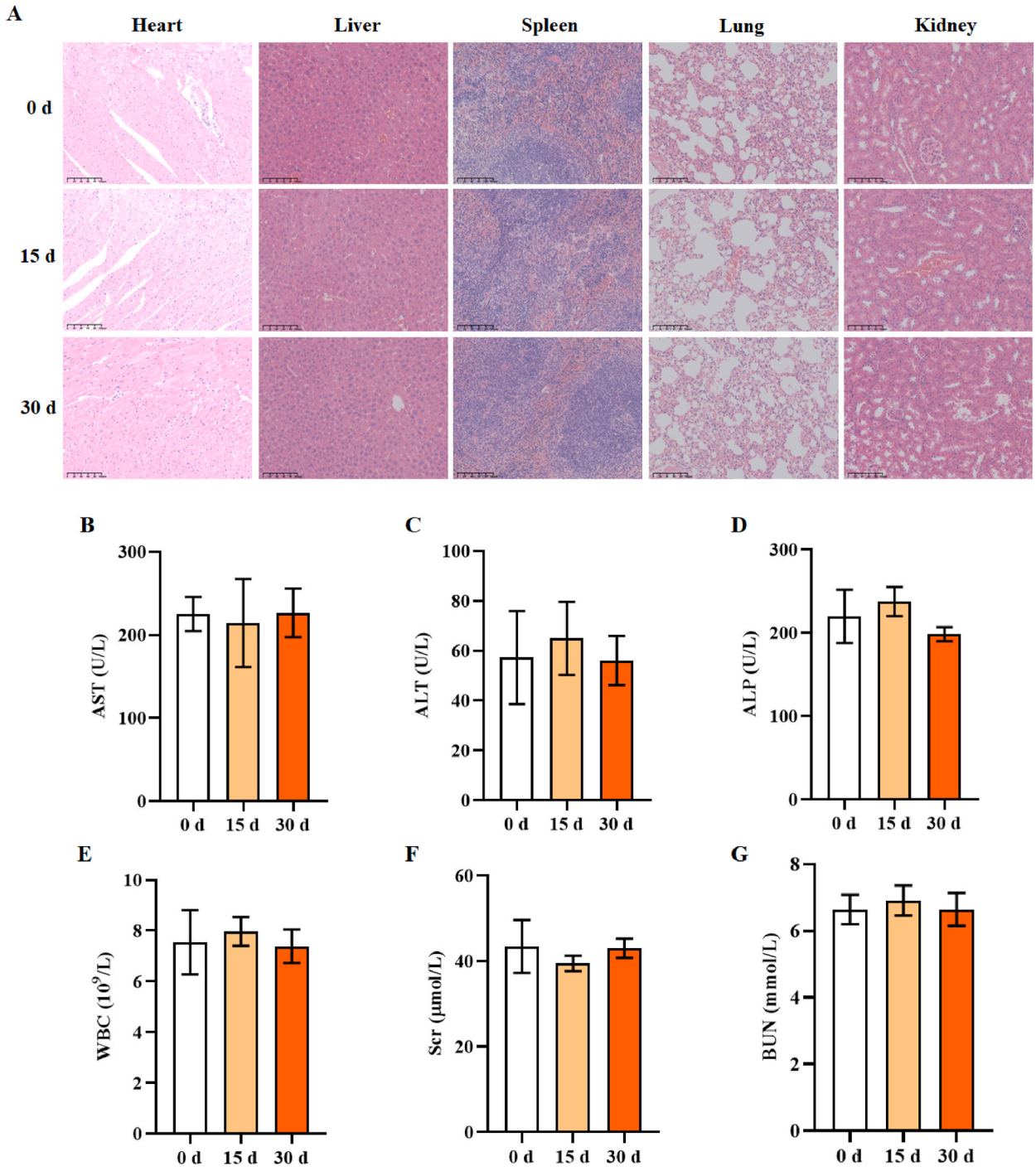

Fig. 6. *In vivo* safety evaluation of TLN. (A) Representative H&E staining of major organs (heart, kidney, lung, liverand spleen). Scale bar = 100 μm. The effects of TLN on AST (B), ALT (C), ALP (D), WBC (E), Scr (F) and BUN (G) in the mice treated with TLN at day 15 and day 30. Data are mean ± SD, n = 3.

production, likely due to increased distribution of NAC in mitochondria.

The early and prominent feature of programmed cell death is the damage of active mitochondria. Mitochondrial damage is characterized by changes in membrane potential and changes in mitochondrial oxidation-reduction potential. The reason for the change of membrane potential may be due to the opening of mitochondrial transition pore, which leads to the entry of ions and small molecules into mitochondria. JC-1 fluorescence probe can reflect the change of mitochondrial membrane potential by varying fluorescence intensity, so as to evaluate the functional state of cells. After incubation with H_2O_2, it was observed that the red/green fluorescence intensity ratio of the cells decreased. This decrease suggests that the oxidative stress induced by H_2O_2 significantly reduced the membrane potential of HK-2 cells. However, when free NAC, LN, or TLN was administered to the H_2O_2-treated cells, the red/green fluorescence intensity ratio noticeably increased. In comparison to LN, the administration of TLN resulted in a greater enhancement of the red/green fluorescence intensity. This suggested that TLN was effective in stabilizing the mitochondrial membrane potential by alleviating oxidative stress in the mitochondria (Fig. 4D). The apoptosis of HK-2 cells was measured by flow cytometry, and the results (Fig. 4E) showed that TLN treatment effectively ameliorated H_2O_2-induced apoptosis.

3.5. TLN alleviates renal dysfunction of AKI mice

In view of the superior ROS scavenging ability *in vitro* and renal distribution, TLN should be effective in IRI-AKI treatment. Scr and BUN are essential measures for assessing renal function and determining the proper functioning of the kidneys. Scr is a byproduct of muscle metabolism and is mainly eliminated through the kidneys. When kidney function is compromised, the levels of Scr increase as the kidneys are unable to efficiently eliminate this waste product. Similarly, BUN is a waste product resulting from protein metabolism and is excreted by the kidneys. In cases where kidney function is impaired, BUN levels experience an elevation. As shown in Fig. 5A and B, Scr and BUN levels were remarkably elevated in IRI-AKI mice compared with sham mice. Compared with free NAC, TLN could significantly reduce the Scr and BUN levels in IRI mice (TLN *vs* free NAC, Scr, 90.3 ± 15.4 *vs* 174.6 ± 17.2 μmol/L, BUN, 9.1 ± 1.4 *vs* 19.6 ± 1.8 mmol/L, $^*P < 0.0001$). Similarly, compared with LN, TLN showed the better therapeutic outcomes (TLN *vs* LN, Scr, 90.3 ± 15.4 *vs* 131.5 ± 15.6 μmol/L, BUN, 9.1 ± 1.4 *vs* 15.5 ± 2.1 mmol/L, $^*P < 0.0001$).

SOD is an enzyme that protects against free radicals. It converts superoxide radicals to hydrogen peroxide and oxygen. MDA is an aldehyde produced from lipid peroxidation. Excessive production of free radicals and impaired antioxidants can cause oxidative stress and damage to cells [14]. IRI occurs when blood flow is interrupted and then restored, leading to oxidative stress. Both SOD and MDA were measured in renal tissues to evaluate the effect of TLN in protecting against kidney damage from oxidative stress. As shown in Fig. 5C and D, TLN treatment effectively ameliorated abnormal levels of SOD and MDA in comparison to that of free NAC and LN (TLN *vs* free NAC, SOD, 136.2 ± 27.0 vs 78.2 ± 18.2 U/mg prot, P = 0.0014; MDA, 1.12 ± 0.4 vs 4.2 ± 1.7 nmol/mg prot, P = 0.0013. TLN *vs* LN, SOD, 136.2 ± 27.0 vs 90.4 ± 18.3 U/mg prot, P = 0.0064; MDA, 1.12 ± 0.4 vs 3.2 ± 0.8 nmol/mg prot, P = 0.0002.)

The pathological changes in renal tissues were examined by H&E staining. As shown in Fig. 5E, the renal tissue of IRI-AKI mice had severe tubular necrosis, luminal congestion, and significant infiltration of neutrophils. In contrast, all renal sections obtained from IRI-AKI mice that were treated with free NAC, LN, or TLN, showed significantly less tubular damage to different extent, and TLN-treated mice showed a slight degree of renal tubular damage. The protein known as KIM-1 is a popular biomarker used in the early detection and diagnosis of injury or damage to the kidneys. Its primary expression is in the proximal tubule cells of the kidney and aids in the repair of damaged tubules. Early detection of kidney damage can be achieved through the use of KIM-1 as a diagnostic tool. Compared with free NAC and LN, TLN effectively reduced the expression of KIM-1 (Fig. 5F and G), as evidenced by the low fluorescence signal. In addition, the expression of KIM-1 in renal tissues was examined by Western blot, and the results showed that TLN treatment could effectively reduce the expression of KIM-1 (Fig. S7). ROS production in renal tissues of IRI-AKI mice after treated with TLN was *in situ* detected by CM-H_2DCFDA staining. As shown in Fig. 5H and I, compared with sham mice, IRI-induced kidney injury increased mitochondrial ROS production after reperfusion, as reflected by the increased H_2DCFDA-positive cells. TLN treatment showed the better ROS scavenging activity than that of free NAC and LN. Those findings support the potential of TLN to alleviate renal damage arising from IRI-AKI, which was benefit from the targeted distribution of TLN in TECs and intracellular mitochondria.

3.6. The in vivo toxicity evaluation

A thorough assessment of the potential toxicity of TLN *in vivo* was conducted, which revealed no significant abnormalities in the H&E staining sections of mice who received treatment with TLN (Fig. 6A). Additionally, relevant biomedical indicators, including AST, ALT, ALP, WBC, Scr, and BUN (Fig. 6B–G), for the mice treated with TLN were found to be normal at day 15 and day 30. Based on these results, it can be concluded that TLN has the potential to be a safe agent for the treatment of IRI-AKI.

4. Discussion

IRI-AKI is a complex condition with oxidative stress being one of its primary causes. The excessive production of ROS lead to several cellular processes like renal injury, inflammation, cytosolic calcium overload, apoptosis/necrosis, and energy depletion. Mitochondria are the major source of intracellular ROS with 90 % of ROS originating in them. Under normal respiratory conditions, mtROS is produced at complexes I and III of electron transport chain (ETC), but it is significantly enhanced during times of stress [15]. After IRI-AKI, ROS production damages mitochondrial proteins and lipids, impairing bioenergetics by disrupting ETC function and increasing mitochondrial membrane permeability. The use of medications to introduce antioxidants can help improve the redox balance, enabling resistance against the harmful effects of ROS. However, it is important to consider the dosage of antioxidants as high

concentrations can actually have a prooxidant effect, causing disturbances in cellular pathways.

NAC, an antioxidant compound, is a colorless, water-soluble amino acid that stabilizes cell membranes and protects collagen and endothelium. NAC plays an important role in maintaining human health. It can resist free radical damage, reduce inflammation and damage in the body, and protect the health of important organs such as the brain, liver and cardiovascular system [11]. In addition, NAC can improve the body's immunity, strengthen the body's resistance to disease [16]. The role of NAC in protecting human health is closely related to its antioxidant properties. NAC can be involved in the synthesis of glutathione, thus helping the body to resist free radical damage and reduce the extent of oxidative stress, at the same time, it can repair the cell and tissue damage caused by excessive free radical activity. In addition, NAC can regulate many important bioactive molecules in the body, including interleukin, tumor necrosis factors and PAF, thus maintaining the chemical balance in the body, it plays an important role in resisting disease and injury. Recent studies have shown that NAC supplementation can have a positive effect on the prevention and improvement of a variety of diseases. For example, NAC can prevent arteriosclerosis and cardiovascular disease, diabetes, cancer, alzheimer's disease and other diseases [17–19]. In addition, NAC can reduce the body's damage and inflammation caused by infection, trauma, surgery and radiation therapy, and improve the quality of life and health. The treatment of IRI-AKI involves targeting oxidative stress, which has been linked to increased morbidity and mortality in end-stage renal disease. Renal endothelial and tubular cells suffer injury due to the significant role played by ROS, and protection against such damage has been exhibited in IRI-AKI models with NAC. However, oral or intravenous administration of NAC poses a challenge as it is easily metabolized, and maintaining an effective drug concentration is difficult. Moreover, adverse side effects like nausea and vomiting are common with high doses of NAC, making its clinical use limited. Thus, it is essential to develop a specific carrier that can target renal tissue for treating renal diseases.

In this study, TLN was designed to deliver the antioxidant NAC to both renal TECs and intracellular mitochondria. We observed that intracellular uptake of TLN in H_2O_2-treated could be significantly enhanced via Megalin receptor-mediated endocytosis. The expression of Megalin receptors was no changed in PBS or H_2O_2-treated cells. Megalin is found in the apical membranes of absorptive epithelia and is highly expressed in the brush border and endocytic vesicles of the proximal tubule for clearing the filtrate and in dense apical tubules for recycling back to the apical membrane. This 600 kDa single transmembrane receptor protein belongs to the low-density lipoprotein receptor family. Its main function is the typical tubular reabsorption of almost all filtered proteins, aiding in the recovery of essential substances that would normally be lost in the urine [20]. Megalin binds to a wide range of ligands, including hormones, signaling molecules, enzymes, and immune-related proteins. It also facilitates the uptake of nephrotoxins such as aprotinin, toxins, aminoglycosides, and chemotherapeutic agents. Furthermore, Megalin receptors act as a receptor for the uptake of heavy metal complexes through its interaction with the transporter protein metallothionein in TECs. *In vivo* biodistribution results showed TLN has special targeting ability to the kidney of IRI-AKI mice. Similarly, no changes in the expression of Megalin receptors were in IRI-AKI mice (Fig. 3A), which assuring the possibility of TLN treatment.

Furthermore, *in vivo* experiments also revealed that the use of polymeric prodrug as a delivery system greatly enhanced the therapeutic benefits of NAC. These benefits include improved kidney function recovery, reduced tubular injury, and alleviation of oxidative stress. The enhanced therapeutic efficacy can be attributed to several factors. Firstly, the polymeric prodrug delivery system ensures the protective circulation of NAC in the blood. Secondly, the addition of LMWC enables targeted drug delivery to the Megalin receptors, resulting in increased accumulation of the drug in TECs. Lastly, the presence of TPP provides the ability to target mitochondria, enhancing drug accumulation in these organelles.

This study also has some limitations. Firstly, the number of experimental samples is limited, and individual differences may affect the experimental results. Secondly, it proves that TLN can improve renal injury indicators to be further increased, such as glomerular filtration rate, inflammatory factors and other indicators. In addition, we can further investigate whether TLN has protective effect on AKI-induced chronic kidney disease.

5. Conclusion

In this study, we designed a delivery system called TLN to transport the antioxidant NAC to renal TECs and intracellular mitochondria. We utilized a simple and stable method for this purpose. At the cellular level, TLN demonstrated low toxicity and effectively eliminated reactive oxygen radicals. It alleviated oxidative stress and prevented cell death caused by H2O2. Furthermore, when administered via tail vein injection, TLN exhibited excellent kidney localization and effectively decreased reactive oxygen species in the kidneys of mice with acute renal failure caused by ischemia reperfusion. TLN also protected the structural integrity of renal functional units, especially renal tubules, and maintained normal renal metabolic function. Comprehensive analyses of pathological sections and blood samples indicated that TLN did not induce acute or long-term toxicity in mice, providing strong evidence for its biological safety. In conclusion, TLN demonstrates a potent ability to scavenge reactive oxygen radicals and holds great potential for minimizing kidney injury and improving clinical outcomes.

Declarations

HK-2 cells (RRID:CVCL 0302) were purchased from Pricella Life Science&Technology Co.,Ltd., and cultured in DMEM/F12 medium supplemented with 10 % FBS and 1 % penicillin/streptomycin, maintained at 37 °C in a humidified atmosphere with 5 % CO_2. All animal experiments in this study were conducted in accordance with the guide for the Care and Use of Laboratory Animals by the Institutional Animal Care and Use Committee of Ningbo Institute of Life and Health Industry and approved by the Experimental Animal Ethics Committee of Ningbo Institute of Life and Health Industry (Permit No. GK-2023-LW-0004).

Data statement

The datasets generated and/or analyzed during the current study are available from the corresponding author on reasonable request.

Funding

This research was supported in part by the Nature Science Foundation of Zhejiang province (LYY19H300001).

CRediT authorship contribution statement

Hao-Le Huang: Writing – original draft, Investigation, Formal analysis. **Cheng Na:** Investigation, Formal analysis. **Can-Xin Zhou:** Supervision. **Jing Liang:** Writing – review & editing, Project administration, Funding acquisition, Conceptualization.

Declaration of competing interest

The authors declare the following financial interests/personal relationships which may be considered as potential competing interests:Jing Liang reports financial support was provided by Nature Science Foundation of Zhejiang province. If there are other authors, they declare that they have no known competing financial interests or personal relationships that could have appeared to influence the work reported in this paper.

Appendix A. Supplementary data

Supplementary data to this article can be found online at https://doi.org/10.1016/j.heliyon.2024.e30947.

References

[1] P.K. Moore, R.K. Hsu, K.D. Liu, Management of acute kidney injury: core curriculum 2018, Am. J. Kidney Dis. 72 (2018) 136–148.
[2] N. Pabla, A. Bajwa, Role of mitochondrial therapy for ischemic-reperfusion injury and acute kidney injury, Nephron 146 (2022) 253–258.
[3] L. Su, J. Zhang, H. Gomez, J.A. Kellum, Z. Peng, Mitochondria ROS and mitophagy in acute kidney injury, Autophagy 19 (2023) 401–414.
[4] F. Di Mario, G. Regolisti, P. Greco, C. Maccari, E. Superchi, S. Morabito, V. Pistolesi, E. Fiaccadori, Prevention of hypomagnesemia in critically ill patients with acute kidney injury on continuous kidney replacement therapy: the role of early supplementation and close monitoring, J. Nephrol. 34 (2021) 1271–1279.
[5] Z. Li, Z. Liu, M. Luo, X. Li, H. Chen, S. Gong, M. Zhang, Y. Zhang, H. Liu, X. Li, The pathological role of damaged organelles in renal tubular epithelial cells in the progression of acute kidney injury, Cell Death Dis. 8 (2022) 239.
[6] P. Hauser, R. Oberbauer, Tubular apoptosis in the pathophysiology of renal disease, Wien Klin. Wochenschr. 114 (2002) 671–677.
[7] E.I. Christensen, H. Birn, T. Storm, K. Weyer, R. Nielsen, Endocytic receptors in the renal proximal tubule, Physiology 27 (2012) 223–236.
[8] R. Nielsen, E.I. Christensen, H. Birn, Megalin and cubilin in proximal tubule protein reabsorption: from experimental models to human disease, Kidney Int. 89 (2016) 58–67.
[9] D.W. Wang, S.J. Li, X.Y. Tan, J.H. Wang, Y. Hu, Z. Tan, J. Liang, J.B. Hu, Y.G. Li, Y.F. Zhao, Engineering of stepwise-targeting chitosan oligosaccharide conjugate for the treatment of acute kidney injury, Carbohydr. Polym. 256 (2021) 117556.
[10] S. Qin, B. Wu, T. Gong, Z.R. Zhang, Y. Fu, Targeted delivery via albumin corona nanocomplex to renal tubules to alleviate acute kidney injury, J. Contr. Release 349 (2022) 401–412.
[11] M. Arakawa, Y. Ito, N-acetylcysteine and neurodegenerative diseases: basic and clinical pharmacology, Cerebellum 6 (2007) 308–314.
[12] M. Zhu, J. He, Y. Xu, Y. Zuo, W. Zhou, Z. Yue, X. Shao, J. Cheng, T. Wang, S. Mou, AMPK activation coupling SENP1-Sirt3 axis protects against acute kidney injury, Mol. Ther. 31 (2023) 3052–3066.
[13] Z. Li, X. Fan, J. Fan, W. Zhang, J. Liu, B. Liu, H. Zhang, Delivering drugs to tubular cells and organelles: the application of nanodrugs in acute kidney injury, Nanomedicine (Lond) (2023).
[14] J.Q. Wu, T.R. Kosten, X.Y. Zhang, Free radicals, antioxidant defense systems, and schizophrenia, Prog. Neuro-Psychopharmacol. Biol. Psychiatry 46 (2013) 200–206.
[15] J.H. Schofield, Z.T. Schafer, Mitochondrial reactive oxygen species and mitophagy: a complex and nuanced relationship, Antioxidants Redox Signal. 34 (2021) 517–530.
[16] B. Kalyanaraman, N.A.C. Nac, Knockin' on Heaven's door: interpreting the mechanism of action of N-acetylcysteine in tumor and immune cells, Redox Biol. 57 (2022) 102497.
[17] Q. Zhu, Y. Xiao, M. Jiang, X. Liu, Y. Cui, H. Hao, G.C. Flaker, Q. Liu, S. Zhou, Z. Liu, N-acetylcysteine attenuates atherosclerosis progression in aging LDL receptor deficient mice with preserved M2 macrophages and increased CD146, Atherosclerosis 357 (2022) 41–50.
[18] Q. Ding, B. Sun, M. Wang, T. Li, H. Li, Q. Han, J. Liao, Z. Tang, N-acetylcysteine alleviates oxidative stress and apoptosis and prevents skeletal muscle atrophy in type 1 diabetes mellitus through the NRF2/HO-1 pathway, Life Sci. 329 (2023) 121975.
[19] J. More, N. Galusso, P. Veloso, L. Montecinos, J.P. Finkelstein, G. Sanchez, R. Bull, J.L. Valdés, C. Hidalgo, A. Paula-Lima, N-acetylcysteine prevents the spatial memory deficits and the redox-dependent RyR2 decrease displayed by an alzheimer's disease rat model, Front. Aging Neurosci. 10 (2018) 399.
[20] S. Goto, Y. Yoshida, M. Hosojima, S. Kuwahara, H. Kabasawa, H. Aoki, T. Iida, R. Sawada, D. Ugamura, Y. Yoshizawa, K. Takemoto, K. Komochi, R. Kobayashi, R. Kaseda, E. Yaoita, S. Nagatoishi, I. Narita, K. Tsumoto, A. Saito, Megalin is involved in angiotensinogen-induced, angiotensin II-mediated ERK1/2 signaling to activate Na + -H + exchanger 3 in proximal tubules, J. Hypertens. 41 (2023) 1831–1843.